Environ Sci Pollut Res (2014) 21:9626–9643
DOI 10.1007/s11356-014-2988-3

RESEARCH ARTICLE

Phragmites sp. physiological changes in a constructed wetland treating an effluent contaminated with a diazo dye (DR81)

Renata Alexandra Ferreira · Joana Gouveia Duarte · Pompilio Vergine · Carlos D. Antunes · Filipe Freire · Susete Martins-Dias

Received: 3 August 2013 / Accepted: 30 April 2014 / Published online: 9 May 2014

Abstract The role of *Phragmites* sp. in phytoremediation of wastewaters containing azo dyes is still, in many ways, at its initial stage of investigation. This plant response to the long-term exposure to a highly conjugated di-azo dye (Direct Red 81, DR81) was assessed using a vertical flow constructed wetland, at pilot scale. A reed bed fed with water was used as control. Changes in photosynthetic pigment content in response to the plant contact with synthetic DR81 effluent highlight *Phragmites* plasticity. *Phragmites* leaf enzymatic system responded rapidly to the stress imposed; in general, within 1 day, the up-regulation of foliar reactive oxygen species-scavenging enzymes (especially superoxide dismutase, ascorbate peroxidase (APX), glutathione peroxidase (GPX) and peroxidase) was noticed as plants entered in contact with synthetic DR81 effluent. This prompt activation decreased the endogenous levels of H_2O_2 and the malonyldialdehyde content beyond reference values. Glutathione S-transferase (GST) activity intensification was not enough to cope with stress imposed by DR81. GPX activity was pivotal for the detoxification pathways after a 24-h exposure. Carotenoid pool was depleted during this shock. After the imposed DR81 stress, plants were harvested. In the next vegetative cycle, *Phragmites* had already recovered from the chemical stress. Principal component analysis (PCA) highlights the role of GPX, GST, APX, and carotenoids along catalase (CAT) in the detoxification process.

Keywords Antioxidant enzymes · Ascorbate–glutathione cycle · Azo dyes · Detoxification · Oxidative stress · Photosynthetic pigments · Phytoremediation

Responsible editor: Elena Maestri

Electronic supplementary material The online version of this article (doi:10.1007/s11356-014-2988-3) contains supplementary material, which is available to authorized users.

R. A. Ferreira · J. G. Duarte · P. Vergine · C. D. Antunes · F. Freire · S. Martins-Dias (✉)
IBB-Institute for Biotechnology and Bioengineering, Instituto Superior Técnico, Universidade de Lisboa, Av Rovisco Pais, 1049-001 Lisboa, Portugal
e-mail: susetedias@tecnico.ulisboa.pt

R. A. Ferreira · J. G. Duarte · F. Freire · S. Martins-Dias
CERENA, Instituto Superior Técnico, Universidade de Lisboa, Av. Rovisco Pais, 1049-001 Lisboa, Portugal

Introduction

Growing environmental pollution resulting from industrial development is one of the main challenges defying the modern world. Discharge of highly coloured effluents due to the presence of man-made dyes has been found to damage the receiving water bodies. Over the years, different physico-chemical treatments were attempted for colour and dyeing compound removal from wastewater. However, these processes have high operational costs and still limited applicability. Dye biodegradation has been focused on bacteria and fungi ability under different redox conditions (Banat et al. 1996; Fu and Viraraghavan 2001; Pearce et al. 2003; Forgacs et al. 2004; van der Zee and Villaverde 2005; dos Santos et al. 2007; Kaushik and Malik 2009; Saratale et al. 2011; Solís et al. 2012). Colour removal is quite fast. An increase in toxicity associated with by-products formed after azo link breakdown has also been observed. Emerging phytoremediation technologies looked promising for the removal and mineralization of synthetic azo dyes from wastewaters; nevertheless, the metabolic aspects of phytoprocesses involved need to be clarified in order to select the appropriate vegetation and optimize the treatment systems.

Plants are unique organisms equipped with remarkable metabolic and absorption skills, along with transport systems that can take up nutrients or contaminants selectively from the

growth matrix, soil or water. Following uptake, the main purpose is to convert the lipophilic xenobiotic into a more water-soluble and less toxic metabolite that can therefore be eliminated (Alkorta and Garbisu 2001). Plant detoxification pathway implicates specific enzymes in three distinct phases. Oxidases (e.g. peroxidases, POD) or oxygenases like P450 a monooxygenase or carotenoid monoxygenases and dioxygenases might be involved in the first transformation step (or phase I). Phase II involves the xenobiotic conjugation by glutathione S-transferase (GST). Finally, in phase III, plant internal compartmentation and elimination of the metabolites formed can be accomplished by storage in the cell vacuole or covalent binding to cell walls (Coleman et al. 1997; Burken 2004; Schröder et al. 2007; Schwitzguébel et al. 2011).

Constructed wetlands (CWs) are engineered lagoons with a natural or impermeable barrier to prevent seepage, filled with a pre-selected soil matrix and vegetation. Wastewater is purified as it flows through the system. To accomplish the effluent treatment with success, vegetation selection should be carried out taking advantage of root exudates, extracellular enzyme production or uptake capabilities (Novais and Martins-Dias 2003). CW hydraulic operation has been described thoroughly by Brix and Schierup (1989). *Phragmites* is one of the most used plants in CW. As a matter of fact, *Phragmites*, in the pilot scale vertical flow constructed wetland (VFCW) that is being used for the treatment of synthetic textile effluents (Davies et al. 2005, 2008), never developed signs of phytotoxicity or abnormal development, indicating that *Phragmites* is able to biochemically self-engineer and therefore play an important role in the detoxification of organic compounds synthetized by man. In previous work, Carias et al. (2008) studied the activities of several enzymes involved in plant protection against stress (antioxidant and detoxification enzymes), evidencing how *Phragmites* adapted to acid orange 7 (AO7) exposure and potential role on degradation pathways.

This study aimed to contribute to the understanding of antioxidant and detoxification mechanisms in *Phragmites* by comparing the changes in specific leaf enzymatic activity in a CW system fed with a high molecular weight (MW≈675.6) di-azo dye with a tap water-fed CW. Direct Red 81 (DR81) was selected as its log Kow (1.65) enables it to be taken up by the plant. Therefore, physiological changes due to natural or induced vegetative cycle and weather conditions could be distinguished from DR81 effects on *Phragmites* physiology. The activation of the detoxification pathway and subsequent DR81 conjugation was considered by means of GST activity. Endogenous hydrogen peroxide (H_2O_2) content and lipid peroxidation, through malonyldialdehyde (MDA) content, were assessed as tools to measure the extent of oxidative stress. Simultaneously, the influence of DR81 on leaf catalase (CAT) activity and photosynthesis was analysed. In order to clarify how a chemical stress event alters *Phragmites* sp. status, the study was carried during 9 months.

Materials and methods

Pilot vertical flow constructed wetland operating conditions

The experimental work was developed using two pilot scale VFCWs (0.96 $m^2 \times 0.87$ m) planted with *Phragmites* sp. installed at Técnico Lisbon University campus and described in previous experiments (Martins Dias 1998; Davies et al. 2005) (Fig. 1). The reed beds were fed in an intermittent pulsed feeding mode eight times a day (12.1±2.5 min, every 3 h) with an average flow rate of 0.54±0.07 L min^{-1} using a dosing pump (SG 140, Colberge Water Systems). This long-term trial was divided into three feeding phases (P_0, P_1 and P_2) for the VFCW1: P_0 comprises a 6-month period (from October to April) pulse-fed with tap water, followed by P_1, a 4-month (until August) feeding with DR81 synthetic effluent, and in P_2, the reed bed was pulse-fed with water for another 4 months (until December). VFCW2 was always pulse-fed with tap water albeit the same three feeding phases are considered for comparative analysis. The VFCWs were harvested in the end of P_1 to impose a second vegetative cycle.

A commercial grade (32 % purity) DR81 (disodium 7-benzamido-4-hydroxy-3-[[4-[(4-sulphonatophenyl) azo] phenyl] azo] naphthalene-2-sulphonate, $C_{29}H_{19}N_5Na_2O_8S$) supplied by U.T. Químicos Unipessoal Lda was selected in order to resemble industrial textile effluent including dissolved salt contents. DR81 impurities are mostly calcium and sodium sulphate salts. Influent batches of 150 L were prepared twice a week at 196±43 mg L^{-1} of DR81 using tap water. DR81 concentration was determined at its maximum visible absorption wavelength (507 nm).

Plant material

Pilot VFCWs have a surface area of ca. 1 m^2 covered with vegetation (>100 plants m^2) (Fig. 1). Influent distribution system over soil surface and hydraulic operating mode assures that all plants are exposed to pollutants during the same time. Leaf sampling procedure involves the collection of the first three leaves of stems higher than 40 cm randomly selected around the VFCW. The first portion of *Phragmites* leaves was cut and immediately frozen in liquid nitrogen. All procedure took less than 20 s per plant sampled. A total of ca. 20 g of leaves per sampling was collected from which ca. 5 g was frozen and the remaining portion used for total Kjeldahl nitrogen (TKN) and humidity quantification.

The first sample was collected from VFCW1 immediately before the 1st pulse-fed cycle with DR81 (0 h) and at the end of the 1st (0.25 h), 2nd (3 h), 9th (24 h), 48th (144 h) and

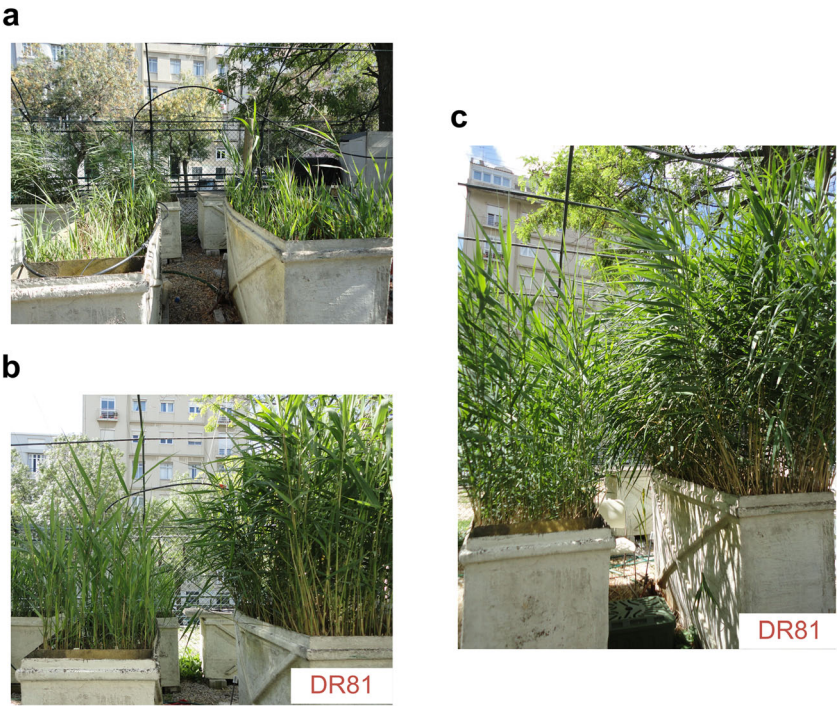

Fig. 1 VFCW pilot reed beds. VFCW1 (on the *right side*) pulse-fed with the synthetic dye (DR81) and VFCW2 (on the *left side*) fed with tap water. Start-up of the trial by the end of March (**a**), mid of May (**b**), end of vegetative first cycle (3rd of August) (**c**)

840th (2,520 h) pulse-fed cycles with the dye. Leaves were also collected at the end of the last pulse-fed cycle with tap water of the second vegetative cycle, P_2, following the previously described procedure, but no young leaves were found. VFCW2 was always simultaneously sampled and used as control.

All leaf samples were ground under liquid nitrogen in a steel mortar and pestle before long-term storage in liquid nitrogen (cryogenic storage system Arpege 40, Air Liquide).

Monitoring of plant growth

The height of 20 plants per VFCW was measured during the experiment. Plants were also visually inspected for toxic signs such as chlorosis, leaf anatomical changes, early senescence stages and plant death.

Leaf total Kjeldahl nitrogen content and moisture

Approximately 500 mg of the dried leaf samples was used for the determination of TKN content following the procedure described in Kalra (1998). Relative concentration was estimated comparatively to TKN content at 0 h. Three independent determinations were performed. Leaf moisture content was quantitatively determined based on the gravimetric loss of free water associated with heating at 105 °C for a period of 2 h (Kalra 1998) in order to express results per unit of leaf dry weight. In general, fresh leaf humidity was ca. 70 % in wet basis (detailed results not shown). TKN content was determined per gram of leaf dry weight to enable full comparison between VFCWs.

Photosynthetic pigments

Photosynthetic pigments (chlorophyll *a*, chlorophyll *b* and total carotenoids) were extracted for 2 h from 25 mg of ground leaf tissue into 4 mL of ethanol (95 %) at room temperature, in the absence of light. After centrifugation at 3,000 rpm for 10 min, the absorbance of the supernatant at 470, 648.6 and 664.2 nm was measured. Pigment content was calculated in milligram per gram fresh weight by applying the absorption coefficient equations described by Lichtenthaler (1987). All assays were performed in triplicate.

Crude extract preparation

All materials used were autoclaved at 121 °C for 15 min, prior to use. High chemical grade reagents and ultra-pure water (Milli-Q, Millipore) were always used. According to the target enzymes, two different methods were used to obtain leaf crude extract (CE): CE_I for POD and CE_{II} for all the other enzymes (superoxide dismutase (SOD), ascorbate peroxidase (APX), glutathione peroxidase (GPX), dehydroascorbate reductase (DHAR), glutathione reductase (GR), CAT and GST).

CE_I was prepared with a cooled 0.5-mM calcium chloride ($CaCl_2$) solution following EPA protocol (EPA 1994) with slight changes. Eight millilitres of ice-cold $CaCl_2$ solution was added to approximately 1 g of fresh ground tissue. Tissue suspension was mixed with a vortex and centrifuged for

10 min at 4,000 rpm and 4 °C. Supernatant was collected into a new test tube and stored on ice. The cell wall pellet remaining in the centrifuge tube was re-suspended with 2.5 mL of $CaCl_2$ solution and centrifuged as before. The supernatant was added to the first collected supernatant and stored on ice for 2 h. The final supernatant was collected and stored at −80 °C in aliquots.

CE_{II} was optimized following Davis and Swanson (2001) protocol including a concentration and desalting step. The extraction buffer (EB) was composed of 50-mM phosphate buffer (pH 7.5) containing 10 mM KCl, 1 mM ethylenediamine tetraacetic acid (EDTA), 5 mM dithiothreitol, 0.5 mM Pefabloc and 25 % (*w*/*w*) polyvinylpolypyrrolidone. Eight millilitres of EB was added to approximately 1 g of ground tissue. The suspension was centrifuged for 20 min at 4,000 rpm and 4 °C (Centrifuge 5810 R, Eppendorf). The remaining supernatant was given a second centrifugation at 24,000 rpm and 4 °C for 90 min (XL-90 Ultracentrifuge, Beckman). This resulting supernatant was passed through a 0.2-μm sterile syringe filter (Acrodisc® Syringe Filters with Supor® Membrane, Pall Corporation) and desalted with PD-10 columns (GE Healthcare) using 0.05-M Tris-acetate buffer (pH 7.0) as equilibration and elution buffer. The protein extract was stored at −80 °C in aliquots. Total protein concentration was determined with Pierce® BCA protein assay kit using bovine serum albumin (BSA) as standard.

Enzymatic activity

Each enzyme substrate concentration was optimized previously towards *Phragmites* leaf (Table 1). Enzymatic activity was measured at 25 °C as described in Table 1. A spectrophotometer (Cary 50 Bio, VARIAN), equipped with a microplate reader with temperature controller, was used to follow absorbance changes. Specific activity is expressed as units of activity per milligram of protein in the CE (U mg^{-1}). All assays were done in triplicate.

H_2O_2 content

Hydrogen peroxide levels were determined according to Bouazizi et al. (2010) with minor changes. Fresh ground leaf tissues (150 mg) were homogenized on an ice bath with 1.5 mL of 0.1 % (*w*/*v*) trichloroacetic acid solution. The homogenate was centrifuged at 12,000*g* and 4 °C for 15 min, and 0.5 mL of the supernatant was added to 0.5-mL potassium phosphate buffer (10 mM, pH 7.0) and 1 mL potassium iodide (1 M). The absorbance of the mixture was measured at 390 nm. The content of H_2O_2 was obtained using a standard curve.

Lipid peroxidation

Lipid peroxidation degree in leaf tissues was assessed by its MDA content, quantified by the thiobarbituric acid test, as described by Velikova and Loreto (2005).

Statistical data analysis

A statistical data analysis was performed using the free software Tanagra 1.4.40. Each VFCW was characterized by chlorophyll *a* (Chl *a*), chlorophyll *b* (Chl *b*), carotenoids (Car), TKN, MDA and H_2O_2 leaf contents and APX, CAT, DHAR, GPX, GR, GST, POD and SOD activities at each selected feeding cycle, here by named attribute. A hierarchical agglomerative clustering (HAC) was used to group data with similar characteristics in clusters. Time and VFCW were expressed as discrete variables, and their distribution amongst the clusters

Table 1 *Phragmites* leaf enzymatic activity quantification protocols. Optimum substrate concentration previously determined and molar extinction coefficients (ε) obtained from literature

Enzymes	Substrates	ε (mM^{-1} cm^{-1})	References
POD	H_2O_2 (0.46 mM)	6.58	EPA (1994); Patil and Speaker (2000)
SOD	NBT (0.12 mM)	–	Carias et al. (2008)
APX	Ascorbic acid (0.5 mM) H_2O_2 (0.46 mM)	2.8	Carias et al. (2008); Miyake and Asada (1996)
GPX	H_2O_2 (0.8 mM)	6.22	Ali et al. (2005)
CAT	H_2O_2 (12 mM)	0.0436	Davis and Swanson (2001); Rad et al. (2007)
GR	NADPH (0.05 mM) GSSG (0.5 mM)	13.6	Davis and Swanson (2001); Mockett et al. (1999)
DHAR	DHA (2.5 mM)	14.7	Carias et al. (2008); May et al. (1997)
GST	GSH (20 mM) CDNB (1.6 mM)	9.6	Habig et al. (1974)

APX ascorbate peroxidase, *CAT* catalase, *CDNB* 1-chloro-2,4-dinitrobenzene, *DHA* dehydroascorbate, *DHAR* DHA reductase, *GPX* glutathione peroxidase, *GR* glutathione reductase, *GSH* glutathione, *GST* glutathione S-transferase, *GSSG* oxidized glutathione, *H_2O_2* hydrogen peroxide, *NADPH* β-nicotinamide adenine dinucleotide phosphate reduced form, *NBT* nitrobluetetrazolium, *POD* peroxidase, *SOD* superoxide dismutase

was evaluated. Test value was determined for each attribute to evaluate its distance to average of all observations of each attribute and the importance of that attribute to the cluster. Test absolute value must be greater than 2 for $p \leq 0.05$.

Afterwards, a principal component analysis (PCA) was applied to each VFCW to identify attributes with similar variance. The number of PCs used to interpret the data was set by the axis eigenvalues (>1). For each PC axis, attributes with an auto value with the same signal are directly correlated, and attributes with auto values with different signal are inversely correlated.

All experimental data sets were tested for normality using Shapiro–Wilk test and SPSS 22.0.0 software. Student's paired t test was used for statistical significance analysis. A significant difference was considered at the level of $p \leq 0.05$.

Results and discussion

VFCW performance

DR81 was successfully removed from the influent as observed in Fig. 2. A small decrease in colour removal efficiency was noticed in the end of the trial from 96 to 89 %. It should be emphasized that a pseudo-stationary phase was achieved in less than 1 week and in the end of P_1, vegetation was already in senescence. Physical parameters confirm the prevailing of an aerobic environment in the VFCW1. Although VFCW conditions are highly aerobic, dissolved oxygen was on average 7.8±1.7 and 7.9±1.5 mg L^{-1} for influent and effluent, respectively. Aerobic conditions were also confirmed by the oxidation–reduction potential (Eh), which ranged from 117±26 in the influent to 196±51 in the outlet. Average conductivity of the influent was 1 dS m^{-1} and pH equal to inlet and around 7. Daily temperature (T) profile varied in 10 °C. Maximum T in summer was 38 °C and minimum in the end of autumn 4 °C. P_1, average air and soil T were 20±5 and 18±2 °C, respectively. COD and TOC removal efficiencies were 90.0± 5.8 and 89.5±7.8 %, respectively. Therefore, DR81 removal should have been accomplished. Two mechanisms could be foreseen in mineralization within the soil and/or taken up by the plant. Soil adsorption after 1 day in operation was expected to be in equilibrium with influent (Freire et al. 2009) although the trial last 4 months in this phase. Soil bacteria and fungi need facultative or anaerobic environment to break azo bonds. Although VFCW conditions are highly aerobic, the occurrence of some anaerobic spots within the bed has been reported to be related to clogging events. Outlet hydraulic profile was monitored during all trial, and no clogging events were noticed (results not shown).

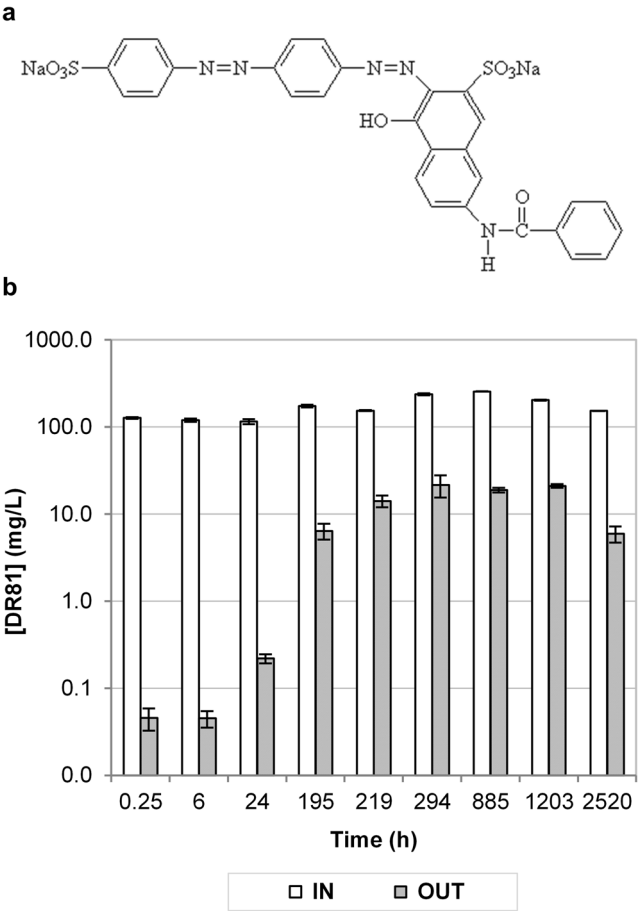

Fig. 2 Chemical structure of the di-azo dye DR81 (**a**) and inlet (IN) and outlet (OUT) dye concentration through the trial (**b**). VFCW was fed every 3 h during 12 min at a flow rate of 0.5 L min^{-1}. Hydraulic load was on average 54 L m^{-2} day^{-1}. Outlet values corresponds to a 3-h cycle composite sample

Influence of exposure to DR81 on plant development

Phragmites is a perennial plant reaching a maximum height of ca. 200 cm by the end of summer (end of life vegetative cycle). Reed beds were side-by-side, under the same atmospheric conditions. The plant height reached a stationary phase at 177±30 cm for VFCW1 and at 162±25 cm for control (Fig. 3). Visual inspection of vegetation revealed no signs of chlorosis symptoms or leaf anatomical changes or even plant death in both reed beds. Plant's growth and greenness status could be observed (Fig. 1) simultaneously with the presence of panicles, which is a characteristic of this species in middle and/or late summer. Results indicate that *Phragmites* development (normal plant life cycle) was affected by the exposure to DR81. In fact, immediately after the start of P_1 and during the first month of this phase, plant's height in VFCW1 was significantly higher ($p \leq 0.05$) when compared

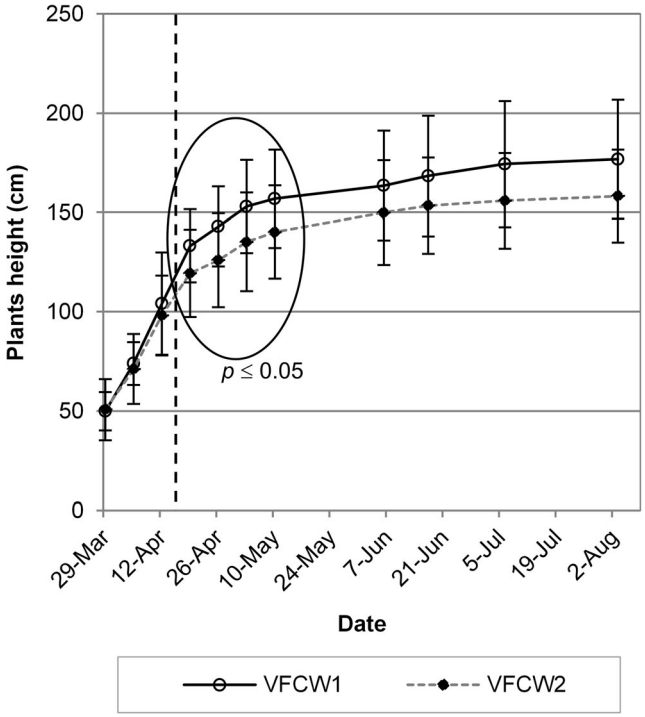

Fig. 3 *Phragmites* sp. growth curves in VFCW1 and VFCW2 (control). *Dashed vertical line* marks the change of feeding source from water to synthetic DR81 effluent in VFCW1. The *elliptical shape* marks the period where the plant's height in VFCW1 was significantly higher ($p \leq 0.05$) when compared to the control

to the control (Fig. 3). This indicates that perhaps *Phragmites* was able to use DR81 as nitrogen source as no other external nitrogen source was available.

During the new vegetative cycle, P_2, growth curve also followed a sigmoid shape (results not shown). Plants reached a growth stationary phase early November, with an equal average height of 168±23 and 147±21 cm for VFCW1 and control, respectively. Once more, some plants in both systems presented panicles. When comparing the two phases of the trial, the slight decrease of height in the plants of both CWs in P_2 was expected since seasonal temperature has a strong influence on shoot growth (Zemlin et al. 2000) turning the interference of the previous feeding with DR81 in the VFCW1 into a null hypothesis.

Comparing *Phragmites* growth dynamics before and after contact with DR81 in opposition to plants that were not in contact with the dye reinforces the capability of this plant species for phytoremediation processes.

HAC analysis

The characterization of the physiological status of *Phragmites* resulted in a large number of data. To acquire a comprehensive overview of the differences imposed by the feeding source on each VFCW, an HAC analysis was carried out. HAC analysis grouped all data in five clusters (Table 2). The importance of each attribute to the cluster is presented in Table 3.

VFCW2 data of the first feeding period of time, P_1, was grouped in cluster I meaning a reference consistent pattern for all variables. Cluster II describes *Phragmites* sp. physiological status in the presence of DR81 revealing that plant was able to adapt to the pollutant by reverting the stress response (cluster III) at the 24-h exposure to DR81, as it includes the 144-h cycle. Cluster II is headed by APX and GR while SOD, Car, CAT, and GST adapt to DR81. Cluster III is characterized by significant changes in GPX and H_2O_2 contents along with POD. Cluster IV was also assigned to VFCW1 at the end of P_1 showing that *Phragmites* may have reached an earlier senescence state comparatively to control. Cluster V grouped both VFCW in the end of the new vegetative cycle (December).

The contribution of each parameter to the overall characterization of the physiological status of *Phragmites* sp. is discussed in the following paragraphs.

Influence of DR81 on *Phragmites* leaf TKN content

After 3 hours in contact with DR81, TKN leaf content reached a maximum (ca. 10 %, $p \leq 0.05$) returning close to the basal level (Table 4) in the next 18 h (Fig. 4). In the end of P_1, it suffered a 10 % decrease ($p \leq 0.05$). In the control, reed bed leaf TKN content remained constant until August when a 20 % reduction ($p \leq 0.05$) was noticed (Fig. 4). Gonzalez-Alcaraz et al. (2012) have found different patterns of accumulation and translocation of nitrogen in *Phragmites* tissues. Considering that in the beginning of P_1, the plants were in an active growth stage (spring), the increase in leaf TKN content in the VFCW1 may be due to the combination of two factors: increase of physiological activity (plant development) and increase of nitrogen availability derived from DR81

Table 2 Cluster organization achieved by HAC data analysis. VFCW1 was intermittently pulse-fed every 3 h for 12 min with DR81 at 196± 43 mg L^{-1}, during P_1 (4 months). VFCW2 (control) was fed with tap water in the same period. During P_2 (3,280 h), both VFCWs were fed with tap water. The intermittent pulse-fed hydraulic regime remained constant during trial for both CWs

Chronological time (h)		Clusters	
		VFCW1	VFCW2
P_1	0	II	I
	0.25	II	I
	3	II	I
	24	III	I
	144	II	I
	2,520	IV	I
P_2	5,800 (Dec.)	V	V

Table 3 Mean value of the attributes in each cluster and corresponding test value

Attribute	Cluster I VFCW2 (0-2520h)		Cluster II VFCW1 (0, 0.25, 3 and 144h)		Cluster III VFCW1 (24h)		Cluster IV VFCW1 (2520h)		Cluster V VFCW1 and 2 (5800 h)		Overall mean value
	Test value	Mean value	Test value	Mean value	Test value	Mean value	Test value	Mean value	Test value	Mean value	
Chl a (mg/gFW)	3.23	1.72 (0.11)	-0.31	1.61 (0.18)	0.41	1.66 (0.08)	-2.19	1.40 (0.09)	-2.85	1.43 (0.16)	1.62 (0.18)
Chl b (mg/gFW)	1.19	0.60 (0.03)	1.39	0.61 (0.06)	1.25	0.63 (0.01)	-4.39	0.43 (0.02)	-1.18	0.56 (0.05)	0.59 (0.06)
Car (mg/gFW)	2.38	0.37 (0.04)	-2.47	0.33 (0.03)	0.12	0.36 (0.01)	1.19	0.38 (0.02)	-1.14	0.34 (0.04)	0.36 (0.04)
TKN (mg/gdw)	1.70	36.47 (2.98)	1.99	37.11 (1.41)	0.97	37.29 (0.40)	-1.45	32.56 (0.79)	-4.63	29.25 (0.78)	35.40 (3.47)
GST (U/mg)	5.28	0.33 (0.02)	-2.48	0.26 (0.01)	0.67	0.30 (0.00)	-3.19	0.20 (0.00)	-2.41	0.24 (0.01)	0.28 (0.05)
SOD (U/mg)	-4.66	11.32 (1.27)	2.64	47.83 (21.32)	2.98	72.94 (0.44)	1.69	55.25 (1.57)	-0.25	29.60 (20.69)	31.90 (24.48)
CAT (U/mg)	4.01	140.55 (9.12)	-2.98	116.89 (6.38)	-0.76	121.85 (9.88)	0.20	130.67 (2.45)	-1.41	120.11 (28.01)	128.83 (16.22)
POD (U/mg)	-3.12	0.02 (0.00)	-0.49	0.02 (0.00)	4.39	0.03 (0.00)	0.05	0.02 (0.00)	1.79	0.02 (0.00)	0.02 (0.00)
GPX (U/mg)	-0.95	1.49 (0.14)	-1.97	1.35 (0.08)	5.87	2.97 (0.10)	-0.90	1.34 (0.03)	0.23	1.60 (0.25)	1.56 (0.43)
APX (U/mg)	0.81	0.70 (0.06)	-3.86	0.60 (0.06)	1.25	0.75 (0.00)	3.84	0.88 (0.01)	0.09	0.69 (0.03)	0.69 (0.09)
DHAR (U/mg)	-1.19	0.15 (0.01)	-1.44	0.15 (0.01)	-0.65	0.15 (0.00)	5.10	0.21 (0.00)	0.27	0.16 (0.01)	0.16 (0.02)
GR (U/mg)	-1.92	0.08 (0.00)	-2.43	0.07 (0.00)	-0.70	0.08 (0.00)	0.83	0.08 (0.00)	5.74	0.10 (0.00)	0.08 (0.01)
H_2O_2 (µmol/gFW)	1.47	0.72 (0.04)	-0.74	0.66 (0.16)	-3.72	0.42 (0.02)	-1.02	0.61 (0.02)	2.37	0.80 (0.03)	0.69 (0.13)
MDA (µmol/gFW)	-1.58	0.01 (0.00)	-1.64	0.01 (0.00)	-1.82	0.01 (0.00)	0.52	0.01 (0.00)	5.31	0.01 (0.00)	0.01 (0.00)

Green cells correspond to a $p \leq 0.05$ (test value >2.0). From August (2,520 h) to December (5,800 h), the two VFCWs were pulse-fed with water (FP2)

uptake. As TKN content on control plants remains unchanged, the later possibility should be taken into account. Indeed, plants are able to elaborate physiological and morphological responses to changes in nitrogen supply in order to adjust their growth and development (Kiba et al. 2011). Nitrogen assimilation is related to the synthesis of glutamine, which will be converted into glutamate mediated by NADH or ferredoxin. Main glutamate metabolic products are amino acids (essential in protein synthesis) and glutathione, critical in oxidative stress regulation (Kissen et al. 2010). At the end of the P_1, leaf TKN content decreased in the two VFCWs, which could be explained by plant senescence and relocation of nitrogen that sank from leaf tissues to the roots (Chapin et al. 1990; Lippert et al. 2001). The same pattern was confirmed at the end of P_2, in December (Fig. 4) for the two CW plants.

Photosynthetic pigment content adaptation to DR81

Photosynthetic molecular mechanism efficiency is maintained at the highest level by plants due to the central role of photosynthesis as an energy source (Rochaix 2011). Therefore, in monitoring the leaf photosynthetic pigment content, the overall plant status was assessed (Table 5). The leaf pigment content of VFCW2 remained unchanged ($p>0.05$) up to the end of P_1. However, *Phragmites* plants that were in contact with DR81 presented important variations on leaf pigment content. After the first 15 min in contact with the dye (0.25 h), all pigments decreased significantly ($p \leq 0.05$). Korte et al. (2000) concluded that the organic toxicant penetration into cytoplasm and subsequent incorporation and accumulation into subcellular organelles occur in the first 30 min, and that could be our case. Nevertheless, *Phragmites* photosynthetic apparatus was able to rapidly adjust and return to the reference values (0 h) after the next feeding batch (3 h). However, after 144-h exposure to DR81, a significant decrease ($p \leq 0.05$) in the Car content was observed. A similar behaviour was reported for duckweed treated with acid blue 92 (Khataee et al. 2012). The pool of Car is controlled in part by the rate of degradation by carotenoid

Table 4 Reference values of *Phragmites* leaf specific enzymatic activity and H_2O_2 and MDA and TKN contents determined at the beginning of P_1 (0 h). Values are a mean of three independent determinations ± standard deviation

	VFCW1	VFCW2
Specific activity (U mg^{-1})		
SOD	31.6±1.1	11.3±0.4
APX	0.59±0.06	0.61±0.01
GPX	1.29±0.03	1.47±0.04
CAT	123.4±0.5	138.4±3.8
POD	0.020±0.001	0.018±0.004
DHAR	0.167±0.004	0.145±0.002
GR	0.074±0.001	0.064±0.002
GST	0.244±0.005	0.322±0.007
Content		
H_2O_2 (µmol g^{-1} FW)[a]	0.83±0.02	0.78±0.01
MDA (µmol g^{-1}FW)[a]	0.0078±0.0004	0.0066±0.0003
TKN (mg g^{-1} DW)[a]	36.12±0.13	38.15±0.26

[a] Values are a mean of three biological replicates ± standard deviation

FW fresh weight, *DW* dry weight

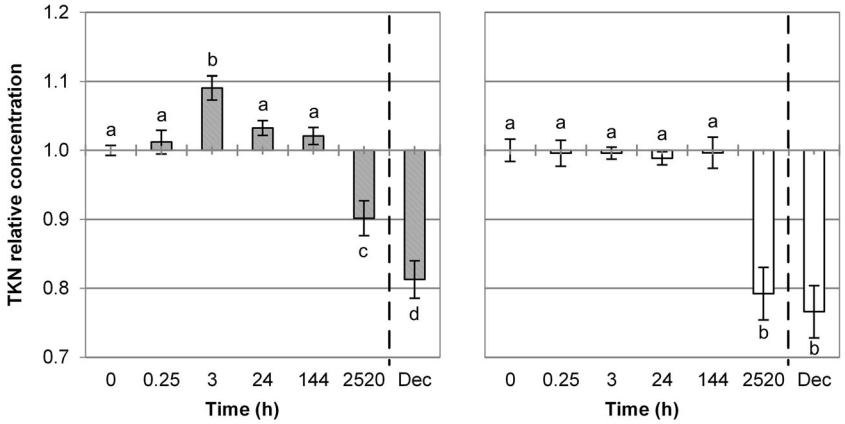

Fig. 4 *Phragmites* sp. leaf TKN relative concentration. *Grey bars* represent data from the VFCW1, pulse-fed with the synthetic dye (DR81), and *white bars* represent data from the VFCW2 (control). *Dashed vertical line* marks the aerial part cut and the beginning of a new vegetative cycle. From August to December (3,280 h), the two VFCWs were pulse-fed with water (FP2). *Error bars* indicate standard deviations (n=3), and values with the same letter are not significantly different at $p \leq 0.05$

cleavage dioxygenases (CCDs). The phytohormone abscisic acid and strigolactones produced by CCD enzymes control abiotic stress-signalling pathways and lateral shoot growth, respectively (Cazzonelli and Pogson 2010; Ha et al. 2014). An increase in lateral shoot growth was also observed in VFCW1 (Fig. 1).

Car main function is photoprotection of the photosynthetic apparatus by quenching triplet chlorophyll, singlet oxygen and other reactive species (Biswal 1995; Vishnevetsky et al. 1999; Blankenship 2002). Car also plays an important structural role as thylakoid membrane stabilizers of the lipid phase (Havaux 1998). A significant reduction in this pigment content finally results in plant death because of the lost photoprotection (Kim et al. 2004). After 144 h of plant exposure to the dye, the Car depletion of 20 % was harmless, as observed by Dankov et al. (2009). Therefore, the excess of singlet oxygen resulting from the Car deficit may constitute the signal transduction that leads to the necessary metabolic

Table 5 Chlorophylls, total carotenoids content and pigment ratios in *Phragmites* leaves collected during the trial from both VFCWs. Values are a mean of three biological replicates ± standard deviation. Statistical differences are indicated by a small letter ($p \leq 0.05$)

Chronologicaltime (h)	Chl *a* (mg g^{-1} FW)	Chl *b* (mg g^{-1} FW)	Car (mg g^{-1} FW)	Chl *a*/*b*	Chl *a*+*b*/Car
VFCW1					
Pulse-fed with DR81(April to August)					
0	1.7±0.1 a	0.6±0.0 a	0.4±0.0 a	2.7±0.0	6.6±0.4
0.25	1.3±0.0b	0.5±0.0 b	0.3±0.0 b	2.5±0.0	5.7±0.4
3	1.7±0.0 a	0.6±0.0 a	0.4±0.0 a	2.8±0.0	6.6±0.2
24	1.7±0.1 a	0.6±0.0 a	0.3±0.0 a	2.6±0.0	6.4±0.3
144	1.7±0.0 a	0.6±0.0 a	0.3±0.0 b	2.6±0.0	7.9±0.5
2,520	1.4±0.0 c	0.4±0.0 c	0.4±0.0 a	3.2±0.0	4.7±0.2
Pulse-fed with water (August to December) and after harvesting					
5,800	1.6±0.0 d	0.6±0.0 a	0.4±0.0 a	2.6±0.0	5.9±0.5
VFCW2					
Pulse-fed with water (April to August)					
0	1.7±0.0 a	0.6±0.0 a	0.4±0.0 a	2.8±0.1	6.7±0.4
0.25	1.7±0.0 a	0.6±0.0 a	0.4±0.1 a	2.8±0.2	6.6±0.4
3	1.7±0.0 a	0.6±0.0 a	0.4±0.0 a	2.9±0.0	6.6±0.1
24	1.7±0.1 a	0.6±0.0 a	0.4±0.0 a	2.8±0.2	6.2±0.2
144	1.7±0.0 a	0.6±0.0 a	0.4±0.0 a	2.7±0.1	6.4±0.2
2,520	1.6±0.0 b	0.6±0.0 a	0.4±0.0 b	3.0±0.1	4.9±0.2
Pulse-fed with water (August to December) and after harvesting					
5,800	1.3±0.0 c	0.5±0.0 b	0.3±0.0 a	2.5±0.1	5.9±0.2

Car total carotenoids, *Chl a* chlorophyll *a*, Chl *b* chlorophyll *b*

adjustments that finally incite the activation of the enzymatic system protecting the plant from oxidative injury. Car depletion was not followed by an increase in MDA content. Indeed, it decreases denoting that the cytosolic ascorbate–glutathione cycle was up-regulated along with POD (Zang and Kirkham 1996) as will be discussed.

In P_2, the pigment content of the leaves collected from the VFCW1 was higher than the pigment content obtained for the VFCW2. This may be due to higher nitrogen availability in this reed bed roots derived from previous dye taken up and translocation. Indeed, the ratio of Chl *a* plus Chl *b* to total Car is similar indicating that the photosynthetic apparatus of reeds was in the same physiological status. In general, in both VFCWs, the overall pigment content is lower in comparison with P_1. The decline in the photosynthetic capacity accompanying leaf senescence is associated with the loss of Rubisco, a major pool of leaf nitrogen, and therefore, a primary target for proteolysis as part of the remobilization phase of the senescence process (Yoo et al. 2003). This result is in accordance with the leaf TKN content decrease presented previously.

Response of *Phragmites* leaf to DR81

All specific enzymatic activities and H_2O_2 and MDA contents are presented as relative values. The results corresponding to 0 h were considered the basal level (Table 4).

Superoxide dismutase

SOD is one of the key enzymes describing cluster I (reference bed) along with GST (the most important one) and CAT. During P_1, after a slight inhibition ($p \leq 0.05$), SOD activity remained at basal levels (Fig. 6).

In the course of P_1 for VFCW1 (Fig. 5), SOD activity starts to augment after the end of the second feeding cycle (3 h) reaching a 2.5-fold increase 6 days after ($p \leq 0.05$) and remained higher ($p \leq 0.05$) than the basal level up to P_1 end. This corroborates the importance of APX on cluster II, in order to control H_2O_2 levels.

The enzyme SOD acts as the first line of defence against ROS by promoting the dismutation of O_2^- to H_2O_2 and oxygen. Therefore, results suggest an increase in ROS production as a consequence of the chemical stress imposed by the dye as previously observed with a concomitant SOD gene expression activation (Carias et al. 2008; Davies et al. 2009). In fact, photosynthetic inhibition at 0.25 h was also observed which could be attributed to an over-reduction of the electron transport chain leading to an alternative pseudo-cyclic electron flow occurrence. This way, electron transfer precedes from water to photosystem I using molecular oxygen as alternative electron acceptor, leading to the formation of O_2^- (Mehler reaction), which can be disproportionate to H_2O_2 via SOD.

SOD activity in VFCW1 (Fig. 5) was higher than that in control reed bed (Fig. 6) in P_2. So, different ROS production rates could be involved despite the fact that the cluster analysis grouped together the two CWs (cluster V).

DR81 influence on ascorbate–gluthathione cycle

Cluster III explains the 24 h in contact with DR81 and highlights the leading role of GPX followed by POD in stress oxidative answer, while H_2O_2 content also contributes to this cluster description (see Table 3). As a matter of fact, 24 h correspond to eighth feeding cycle and thus to a first equilibrium between DR81 concentration in liquid and soil phase within the reed bed. One day after the plants started to be in contact with DR81, a 2.3-fold increase in the GPX activity was noticed (Fig. 5). For control, GPX remained almost constant through P_1 (Fig. 6). At the end of this phase, GPX activity returns to the basal level in VFCW1 (Fig. 5) and significantly increased ($p \leq 0.05$) in control (Fig. 6). While SOD converts superoxide radical into H_2O_2, CAT and GPX convert H_2O_2 into water. GPX requires several secondary antioxidant enzymes (GR and glucose-6-phosphate dehydrogenase) to regenerate its cofactor glutathione (GSH), NADPH and glucose 6-phosphate. As GR remained unaltered, an excess of glutathione is foreseen due to DR81 uptake and degradation followed by nitrogenous by-product assimilation. In the end of P_1, GR activity increased due to the need of GSH regeneration from oxidized glutathione driven by nitrogen translocation to the root system. Moreover, GPX reduces H_2O_2 and lipid peroxides to water and lipid alcohols, and that could explain the reduction observed in MDA content, as will be discussed.

SOD is highly activated at 144 h, but APX is inhibited beyond the basal levels ($p \leq 0.05$; Fig. 5). That indicates that APX was not the main scavenger of H_2O_2. APX is thought to play an essential role in the scavenging of H_2O_2 in ascorbate–glutathione cycle (Fig. 7) and water–water cycle using ascorbate (ASC) as electron donor. DHAR enzyme is responsible for ASC regeneration using GSH as substrate. DR81 degradation is expected to release amino groups, as consequence of azo link breakdown, which are easily converted into ammonia. Ammonia in excess could be buffered by cytosolic monoxygenases producing NH_2OH, which oxidation by APX in the presence of H_2O_2 inhibits the Mehler peroxidase cycle (Chen and Asada 1990) leading to a depletion of the ASC cell pool. NH_2OH is also an antioxidant that easily scavenges ROS. ASC is also a cofactor of different

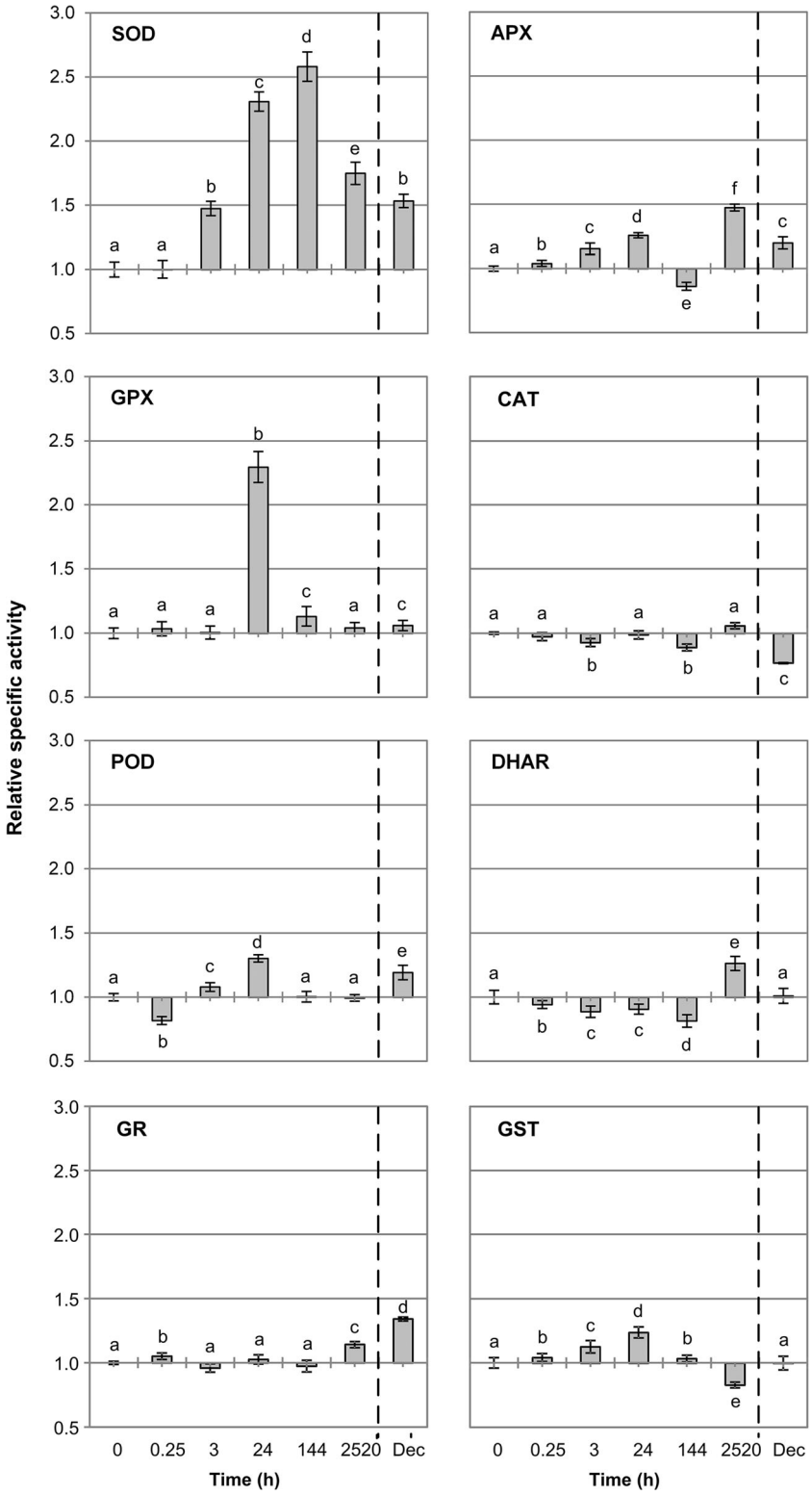

Fig. 5 *Phragmites*' leaves relative specific enzymatic activities in VFCW1 (DR81). *Dashed vertical line* marks the aerial part cut and the beginning of a new vegetative cycle. From August (2,520 h) to December (5,800 h), the twoVFCWs were pulse-fed with water (FP2). *Error bars* indicate standard deviations (n=3), and values with the same letter are not significantly different at $p \leq 0.05$

dioxygenase reactions including Car regeneration (Potters et al. 2002).

At the end of P_1, APX activity rises 47 % when compared to the basal level ($p \leq 0.05$). This maximum value follows an increased regeneration activity of ASC by DHAR and GR. In fact, SOD and APX are the only ROS-scavenging enzymes active at this time (Fig. 5) denoting their importance on *Phragmites* leaf ROS elimination.

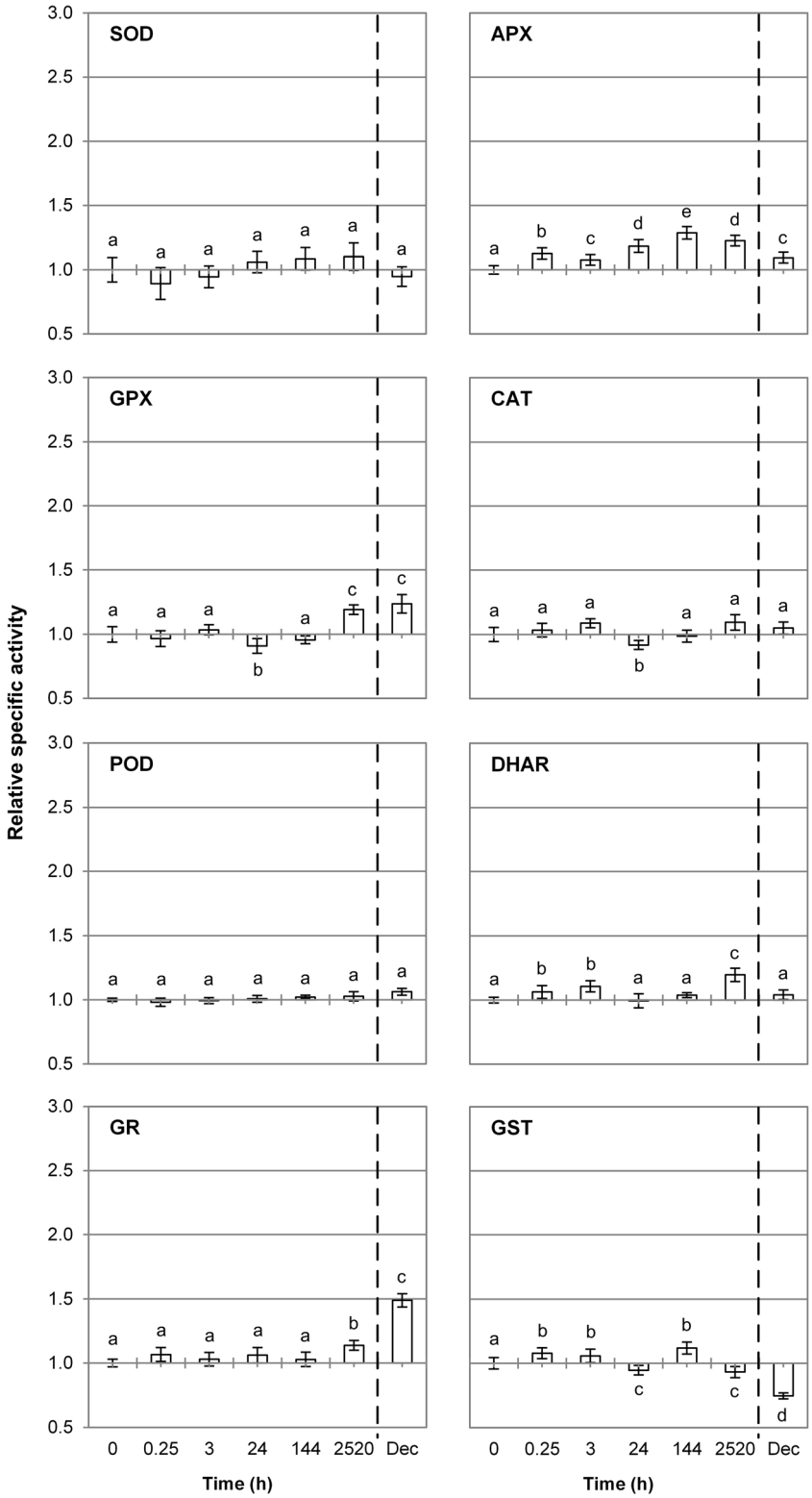

Fig. 6 *Phragmites*' leaves relative specific enzymatic activities in VFCW2 (control). *Dashed vertical line* marks the aerial part cut and the beginning of a new vegetative cycle. From August (2,520 h) to December (5,800 h), the twoVFCWs were pulse-fed with water (FP2). *Error bars* indicate standard deviations (n=3), and values with the same letter are not significantly different at $p \leq 0.05$

In December, the activities of APX, GPX, DHAR and GR enzymes are similar in the two reed beds (Figs. 5 and 6). Nevertheless, GR presented a significant intensification of the activity ($p \leq 0.05$) possibly required for GSH regeneration.

The combined analysis of APX, DHAR and GR activities (Figs. 5 and 6) confirmed the synergy between these enzymes and the use of the ascorbate–glutathione cycle in the elimination of the produced ROS in both VFCW.

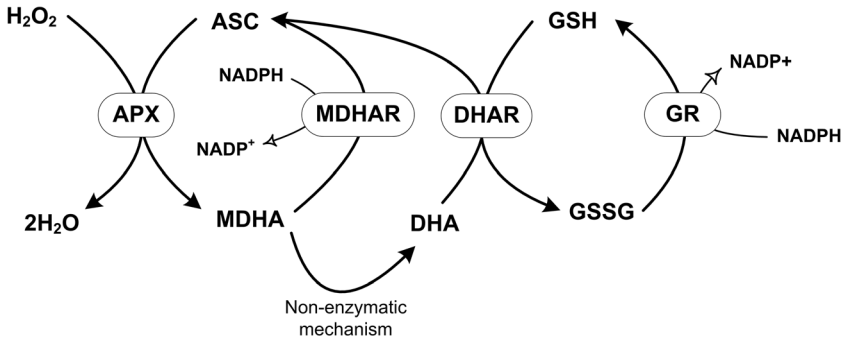

Fig. 7 Schematic representation of the ascorbate–glutathione cycle in the stroma, cytosol, mitochondria and apoplast, adapted from Noctor and Foyer (1998). *APX* ascorbate peroxidase, *ASC* ascorbate, *MDHA* monodehydroascorbate, *MDHAR* monodehydroascorbate reductase, *DHA* dehydroascorbate, *DHAR* dehydroascorbate reductase, *GR* glutathione reductase, *GSH* reduced glutathione, *GSSG* oxidized glutathione

Influence of DR81 on POD activity

POD defines cluster I (reference) and cluster III, the chemical stress moment (Table 3), which means that its activity is not strictly related with DR81 presence. Nonetheless, in the VFCW1, a maximum specific activity (1.3-fold increase) was attained after the first 24 h, but 5 days later, POD reached again control levels and remained constant (Fig. 5). In the same period of time, no changes were observed in control, Fig. 6. Similar peaked response was obtained in the past (Davies et al. 2009). Recently, Khataee et al. (2012) reported that PODs were induced during the decolourization of mono azo acid blue 92 by duckweed plants. Leaf PODs have also been described as a commercial alternative source for the decolourization of textile azo dyes (Shaffiqu et al. 2002). DR81 taken up by *Phragmites* may be easily translocated from roots to shoots and leaves due to its lipophilicity (Barac et al. 2004). Thus, its metabolism in leaf tissues mediated by POD leaf enzymes should be clarified.

In December, P_2, the enzymatic equilibrium changed. Cluster V is driven by GR independently of POD being activated in VFCW1. MDA also defines the cluster, which could mean that GR is not regenerating GSH at the needed rate and lipid peroxidation is taking place or GPX is no longer able to degrade lipid peroxidation by-products.

CAT inhibition by DR81

In VFCW2, CAT activity stayed almost unchanged throughout the trial (Fig. 6). On the other side, CAT is inhibited in the VFCW1 despite the decrease in H_2O_2 content observed (Fig. 8). In fact, after the second pulse-fed cycle (3 h), CAT activity decreased 23 % ($p \leq 0.05$). This was an unexpected behaviour since it was observed previously that CAT activity increased simultaneously with SOD (Carias et al. 2008). CAT is located in peroxisomes and uses either molecular oxygen to remove hydrogen from some organic substrates (peroxidation) producing H_2O_2 or uses H_2O_2 as substrate producing water and molecular oxygen. DR81 or its degradation by-products could have been oxidized by CAT, leading to an accumulation of H_2O_2, hence inhibiting CAT activity. In this case, peroxisome membrane could have been compromised and H_2O_2 dismutated by cytosolic APX.

Moreover, Davis and Swanson (2001) point out that the induction or stimulation of other efficient H_2O_2 scavengers, like GPX and POD, was sufficient to regulate the plant response to the chemical stress imposed. Therefore, CAT was not activated due to plant leaf enzymatic system adaptability. Scandalios et al. (1997) also suggested that fluctuations in H_2O_2 levels play a significant signalling role in the expression of different CAT genes in maize corroborating that CAT was not activated due to the low levels of H_2O_2 within the cell.

Is GST detoxifying?

GSTs are one of the most important groups of detoxification enzymes, which catalyse conjugation reactions between a variety of electrophilic compounds and GSH. DR81 molecular structure contains two azo bonds that theoretically are electrophilic sites that enable conjugation with GSH. From the results obtained (Figs. 5 and 6), it is noticeable the GST activity increases ($p \leq 0.05$) after the first pulse-fed cycle (0.25 h) and up to the eighth pulse-fed cycle (24 h), corresponding to 1.2-fold enrichment (Fig. 5). However, 5 days later, GST activity values were similar to those obtained after the first feeding pulse. The rapid and evident GST response to the new conditions suggests the activation of the detoxification pathway and eventual subsequent dye conjugation. GST was down-regulated after 2,520 h in exposure to DR81. This was probably due to the adaptation of the plant system to the feeding conditions or to lack of GSH for conjugation as a result of their use in the ascorbate–glutathione cycle.

GST changes in VFCW2 during P_1 were considered the normal behaviour of this plant enzyme during the plant vegetative life cycle (Fig. 6). Yet, in P_2, a 25 % inhibition on this enzyme activity was noticed (Fig. 6). GSH depletion can also be the reason for the GST activity decay in the control reed bed

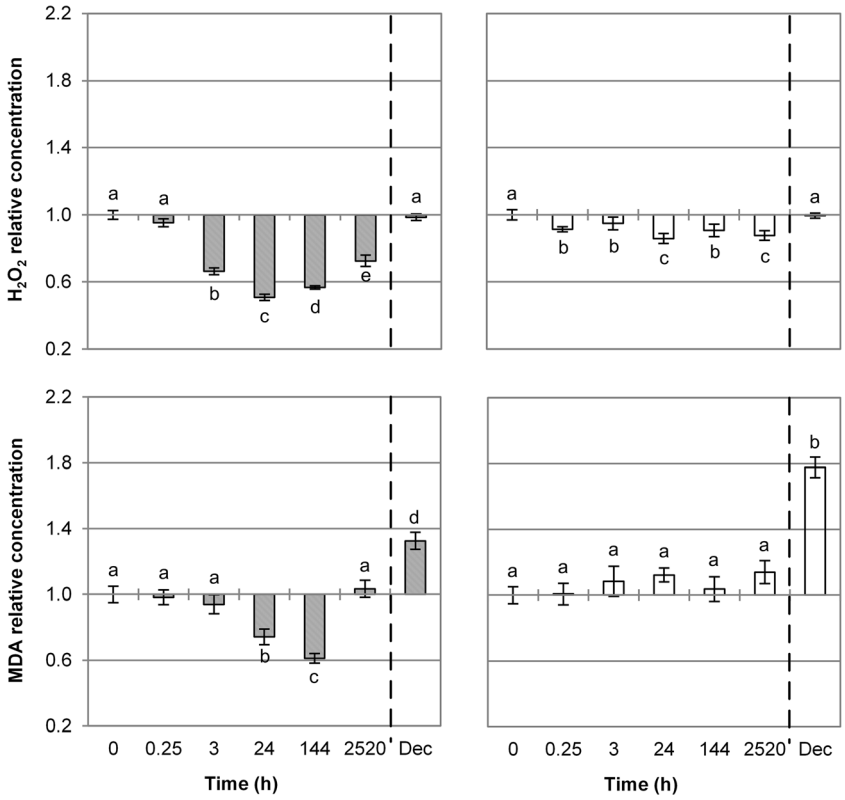

Fig. 8 VFCW1 and VFCW2 *Phragmites*' leaf relative concentration of endogenous H_2O_2 and malonyldialdehyde (MDA). *Grey bars* represent data from the VFCW1, pulse-fed with the synthetic dye (DR81), and *white bars* represent data from the VFCW2 (control). *Dashed vertical line* marks the aerial part cut and the beginning of a new vegetative cycle. From August (2,520 h) to December (5,800 h), the two VFCWs were pulse-fed with water (FP2). *Error bars* indicate standard deviations (n= 3), and values with the same letter are not significantly different at $p \leq 0.05$

during this phase. In December, GST activity was at the basal level ($p>0.05$) in VFCW1 (Fig. 5).

As GST is involved in xenobiotic detoxification and the uptake of dye by the plant is likely, the observed increase in GST activity in VFCW1 was expected when the feeding source was changed from water to synthetic DR81 effluent.

From HAC analysis, GST is an important attribute for all clusters except cluster III. That could mean that despite its peaked activity increase, it was beyond the needed level to cope with DR81 stress.

Phragmites leaf endogenous H_2O_2 content

Sustaining the H_2O_2 content at a proper level can promote plant development and reinforce resistance to environmental stressors (Quan et al. 2008). Low ROS content is known to be required for plant signalling, growth and development (Foyer and Noctor 2000; Mittler 2002), and it orchestrates programmed cell death at high concentrations (Quan et al. 2008). *Phragmites* is a well-studied plant; yet, a foliar endogenous H_2O_2 content for this plant species planted in a CW and under non-controlled biotic factors was not reported so far. *Phragmites* young leaf endogenous H_2O_2 content just before trial (0 h) was 87.8±0.6 μM H_2O_2 and 79.7±1.4 μM for VFCW1 and VFCW2, respectively (Table 4). Foyer and Noctor (2000) reported steady-state levels of 100 to 300 μM of total foliar H_2O_2 concentration, under normal growth conditions. However, variations in H_2O_2 content between plant species, or even in a single species under optimal conditions, can vary more than three orders of magnitude (Cheeseman 2006).

The relative concentration of foliar endogenous H_2O_2 diminishes in the course of the trial (Fig. 8). In fact, 1 day after feeding with DR81, a reduction of nearly 50 % ($p \leq 0.05$) of H_2O_2 content was obtained (this fact was also preponderant in cluster III grouping, see Table 3). This H_2O_2 reduction is in accordance with the up-regulation of APX, GPX and POD, thus emphasizing their active role in H_2O_2 scavenging. The endogenous H_2O_2 foliar content was at the basal level ($p>0.05$) in December. H_2O_2 content in VFCW2 was considered the pattern physiological response of *Phragmites*, under normal growth conditions.

Cell membrane lipid peroxidation

High concentrations of pollutants can increase the permeability of cell membranes and catalyse lipid peroxidation, which can eventually lead to a malfunctioning membrane system. In order to assess the potential membrane damage caused by synthetic textile wastewater, the MDA content of leaf was estimated. Actually, as shown in Fig. 8, in the VFCW1, the MDA content began to decline 1 day after the change of the feeding source from water to synthetic DR81 achieving a significant reduction ($p \leq 0.05$) of ca. 40 % 5 days later but

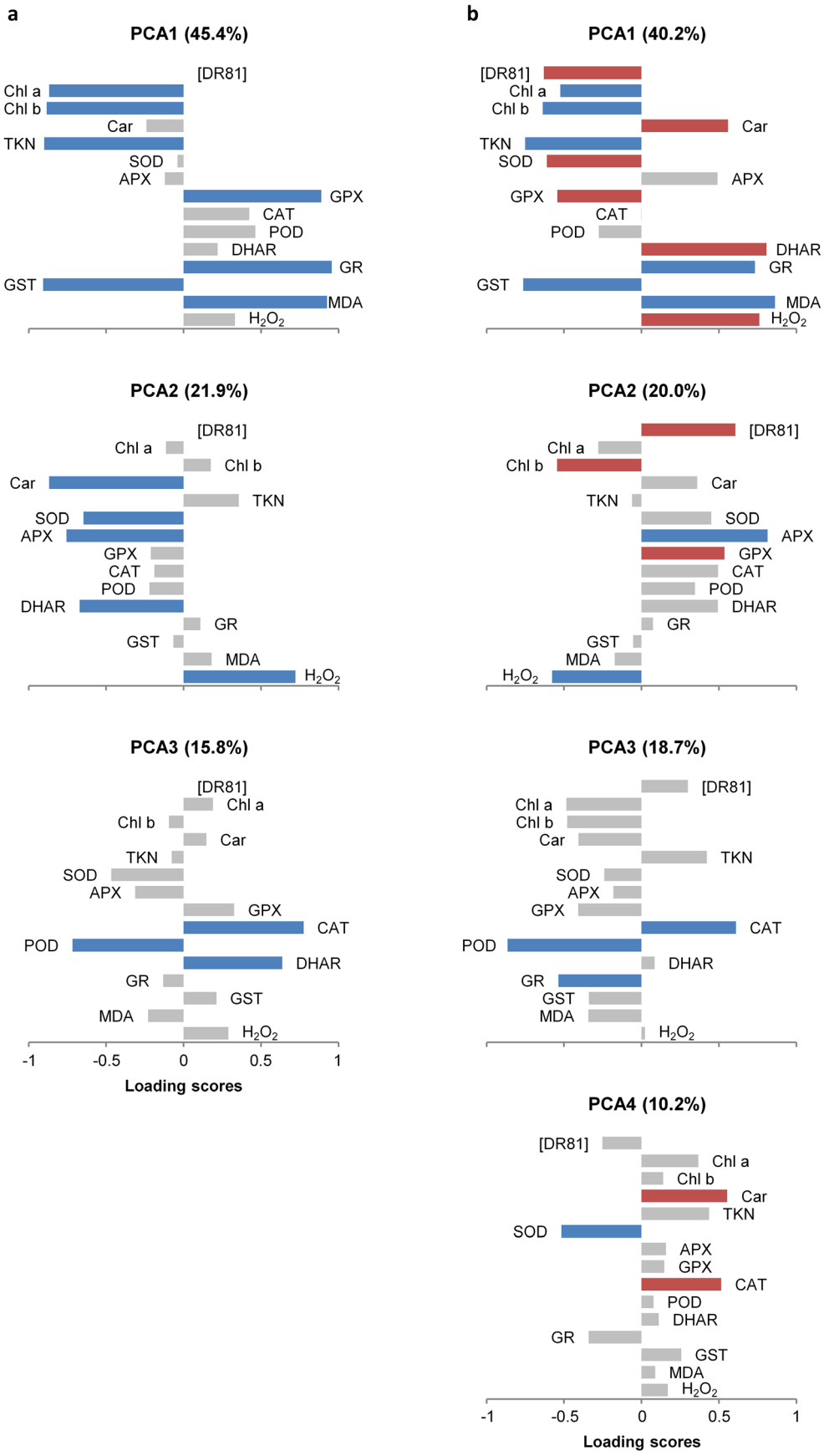

Fig. 9 PCA loadings for the principal components resulting from PCA of VFCW2 (**a**) and VFCW1 (**b**). Attributes that are not well correlated with PCA axis are *grey* and attributes well correlated are *blue*. The *red bars* in **b** show considerable differences between PCA of the two reed beds

returned to the basal level at the end of P_1. In the control system, no significant variations ($p>0.05$) were obtained.

MDA is an end product derived from the decomposition of polyunsaturated fatty acids of biomembranes. Under abiotic stress, lipid peroxidation in *Phragmites* leaf tissues was observed resulting in accumulation of MDA (Fürtig et al. 1999; Velikova and Loreto 2005; Velikova et al. 2005; Xu et al. 2010). However, the observed activation of antioxidant-scavenging enzymes decreased the endogenous levels of ROS species in *Phragmites* leaves and therefore, avoided lipid peroxidation occurrence during P_1. In December, the MDA content of both VFCWs significantly increased ($p\leq0.05$). In fact, the high MDA content of *Phragmites* leaves in December has a preponderant weight in cluster V (see Table 3). Lipid peroxidation has been implicated in programmed cell death, which is an important mechanism of leaf senescence. Previously reported results also indicated that plants were in the final stage of their life cycle; consequently, the MDA accumulation on leaf tissues was expected and confirmed.

Principal component analysis

PCA analysis was applied to each reed bed in order to comprehend if the relation between attributes had been actually modified in VFCW1 due to the pulse-fed with DR81. Matrix covariance eigenvalues and selected axis for each VFCW can be found in supplementary material (Table S1).

VFCW2's data variance (83.1 %) is described by three axes (Fig. 9a). As can be seen in PCA1, the contents of Chl *a*, Chl *b* and TKN are directly correlated with GST; these attributes are also indirectly related with the GPX and GR enzymes. Indeed, all parameters contribute to GSH availability within the cell. GSH synthetized via glutamate also competes with chlorophyll synthesis (Ogawa et al. 2004; Kissen et al. 2010). MDA content, GR and GPX are considered under equilibrium. PCA2 shows that Car content, APX, SOD and DHAR sit together and are oppositeto H_2O_2 content, which was expected (water–water cycle, in chloroplasts). PCA3 analysis indicates that CAT and DHAR are related. Thus, the two ROS-scavenging mechanisms, enzymatic (CAT) and non-enzymatic by ascorbic acid may be cooperating and DHAR involved in the production of ascorbic acid (Rizhsky et al. 2002). Additionally, CAT and DHAR are negatively correlated to POD, which reinforce the high degree of plasticity of plant defence system.

Four axes describe data variance (89.1 %) in VFCW1 (Fig. 9b). PCA1 analysis indicates that DR81 concentration had an impact in the relations between the attributes under study. SOD and GPX are now directly related to DR81 concentration, and H_2O_2 content became an important attribute in the opposite site as expected due to the imposed oxidative stress and in accordance with our previous results (Davies et al. 2009). DHAR and Car present an important direct correlation with H_2O_2 content, which denotes that non-enzymatic mechanisms are playing a role in plant answer to stress. CAT is also related to Car as can be seen in PCA4 (Fig. 9b) competing with SOD; although only 10.2 % of the sample variance is presented in this axis, it corresponds to cluster II, as can be observed in Table 3. Thus, it may constitute the first line of defence. PCA2 and PCA3 reflect the competition between GSH and chlorophyll synthesis from glutamate and the central role of glutamine/glutamate in plant metabolism (for review, view Kissen et al. 2010). Further research is required to address Car content and CAT correlation since it seems to be a function of abiotic stress magnitude (Bouvier et al. 1998; Pradhan et al. 2013).

According to the obtained results, a general explanation for the degradation of DR81 by *Phragmites* is possible. The changing of the feeding source from water to synthetic DR81 effluent disturbed the photosynthetic apparatus of the plant and may have conducted to an increase in the ROS rate production within leaf cells. Concomitantly, and due to the fact that ROS are toxic to the cells, antioxidant-scavenging enzymes are activated. SOD acts as the first line of defence by rapidly converting superoxide radicals in H_2O_2, which will be then converted to water and oxygen by APX, POD and GPX, being this last enzyme identified, by PCA analysis, as having the pivotal role. This analysis also points out the relation of Car and CAT activity, which needs further clarification. Carotenoids are well-known antioxidants and have been emphasized as playing an active role in the abiotic stress signalling being converted into ABA by CCD. In this case, it seems that this signalling strategy was activated. The prompt and over-reaction of the enzymatic antioxidant system culminate with an overall decrease in endogenous H_2O_2 and MDA content, and thus, cell membrane integrity was maintained. A visible proliferation in the number of shoots in the VFVW1 in the end of the first phase of the trial was obtained along with TKN content increase before senescence.

PCA analysis confirms that in parallel, through the detoxification pathway, DR81 should have been transformed, conjugated and assimilated to some extent by the action of GST and GPX within the plant cells. Assumption is corroborated by the high DR81 removal efficiencies from the effluent obtained during more than 2,500 h.

Conclusion

The up-regulation of foliar ROS-scavenging enzymes, especially SOD, APX, GPX and POD, as plants is confronted with synthetic DR81 effluent, clearly indicating that DR81 acts as a plant chemical stressor agent and points out the involvement of *Phragmites* in dye decolourization. The importance and synergy between these enzymes and the use of the ascorbate–glutathione cycle as an antioxidant mechanism were crucial.

Carotenoid involvement in early signalling was observed and to some degree in the increase of shoot density.

Phragmites leaf enzymatic system responded to the stress imposed within 24 h, and a response pattern has been established through HAC analysis. This rapid antioxidative reaction fostered the decreasing of endogenous H_2O_2 and MDA content of *Phragmites* leaf tissues assuring cell membrane integrity.

It is also important to highlight that contrary to our previous results obtained, when the VFCW was pulse-fed with AO7, CAT was not activated, which should be clarified.

The rapid and evident response of *Phragmites* leaf GST to the new feeding source suggests the activation of the detoxification pathway and subsequent DR81 conjugation.

Concurrently, the assessment of the physiological reaction of *Phragmites* revealed normal plant growth with absence of toxic signs or depletion of leaf nitrogen content. Early changes in photosynthetic pigments content in response to the plant contact with synthetic DR81 effluent stress imposed by the dye were rapidly overcome and revealing that they are in line with the antioxidant system. In fact, the up-regulation of SOD arose after photosynthetic inhibition occurrence. SOD activity reaches its maximum when Car depletion was noticed and CAT activity was lower. The excess of singlet oxygen resulting from the Car deficit may constitute the signal for the activation of the enzymatic system.

Acknowledgments The authors acknowledge support from the Fundação para a Ciência e a Tecnologia (SFRH/BD/38704/2007, SFRH/BDE/33911/2009 and PTDC/AAC-AMB/112032/2009). We also thank two anonymous reviewers whose constructive comments helped us improve the overall quality of our manuscript.

References

Ali MB, Hahn E-J, Paek K-Y (2005) Effects of temperature on oxidative stress defense systems, lipid peroxidation and lipoxygenase activity in *Phalaenopsis*. Plant Physiol Biochem 43(3):213–223

Alkorta I, Garbisu C (2001) Phytoremediation of organic contaminants in soils. Bioresource Technol 79(3):273–276

Banat IM, Nigam P, Singh D, Marchant R (1996) Microbial decolorization of textile-dyecontaining effluents: a review. Bioresource Technol 58(3):217–227

Barac T, Taghavi S, Borremans B, Provoost A, Oeyen L, Colpaert JV, Vangronsveld J, van der Lelie D (2004) Engineered endophytic bacteria improve phytoremediation of water-soluble, volatile, organic pollutants. Nat Biotechnol 22(5):583–588

Biswal B (1995) Carotenoid catabolism during leaf senescence and its control by Light. J Photochem Photobiol B 30(1):3–13

Blankenship RE (2002) Molecular mechanisms of photosynthesis. Blackwell Science, Oxford

Bouazizi H, Jouili H, Geitmann A, El Ferjani E (2010) Copper toxicity in expanding leaves of *Phaseolus vulgaris* L.: antioxidant enzyme response and nutrient element uptake. Ecotox Environ Safe 73(6): 1304–1308

Bouvier F, Backhaus RA, Camara B (1998) Induction and control of chromoplast-specific carotenoid genes by oxidative stress. J Biol Chem 273(46):30651–30659

Brix H, Schierup HH (1989) The use of aquatic macrophytes in water-pollution control. Ambio 18(2):100–107

Burken JG (2004) Uptake and metabolism of organic compounds: green-liver model. In: McCutcheon SC, Schnoor JL (eds) Phytoremediation: transformation and control of contaminants. John Wiley & Sons, Inc, Hoboken, pp 59–84

Carias CC, Novais JM, Martins-Dias S (2008) Are *Phragmites australis* enzymes involved in the degradation of the textile azo dye acid orange 7? Bioresource Technol 99(2):243–251

Cazzonelli CI, Pogson BJ (2010) Source to sink: regulation of carotenoid biosynthesis in plants. Trends Plant Sci 15(5):266–274

Chapin FS, Schulze ED, Mooney HA (1990) The ecology and economics of storage in plants. Annu Rev Ecol Syst 21:423–447

Cheeseman JM (2006) Hydrogen peroxide concentrations in leaves under natural conditions. J Exp Bot 57(10):2435–2444

Chen GX, Asada K (1990) Hydroxyurea and p-Aminophenol are the suicide inhibitors of Ascorbate Peroxidase. J Biol Chem 265(5): 2775–2781

Coleman J, Blake-Kalff M, Davies E (1997) Detoxification of xenobiotics by plants: chemical modification and vacuolar compartmentation. Trends Plant Sci 2(4):144–151

Dankov K, Busheva M, Stefanov D, Apostolova EL (2009) Relationship between the degree of carotenoid depletion and function of the photosynthetic apparatus. J Photochem Photobiol B: Biol 96(1):49–56

Davies LC, Carias CC, Novais JM, Martins-Dias S (2005) Phytoremediation of textile effluents containing azo dye by using *Phragmites australis* in a vertical flow intermittent feeding constructed wetland. Ecol Eng 25(5):594–605

Davies LC, Pedro IS, Ferreira RA, Freire FG, Novais JM, Martins-Dias S (2008) Constructed wetland treatment system in textile industry and sustainable development. Water Sci Technol 58(10):2017–2023

Davies LC, Cabrita GJM, Ferreira RA, Carias CC, Novais JM, Martins-Dias S (2009) Integrated study of the role of *Phragmites australis* in azo-dye treatment in a constructed wetland: From pilot to molecular scale. Ecol Eng 35(6):961–970

Davis DG, Swanson HR (2001) Activity of stress-related enzymes in the perennial weed leafy spurge (*Euphorbia esula* L.). Environ Exp Bot 46(2):95–108

dos Santos AB, Cervantes FJ, van Lier JB (2007) Review paper on current technologies for decolourisation of textile wastewaters: perspectives for anaerobic biotechnology. Bioresource Technol 98(12): 2369–2385

EPA (1994) Plant peroxidase activity determination, SOP#: 2035. United States Environmental Protection Agency

Forgacs E, Cserháti T, Oros G (2004) Removal of synthetic dyes from wastewaters: a review. Environ Int 30(7):953–971

Foyer CH, Noctor G (2000) Oxygen processing in photosynthesis: regulation and signalling. New Phytol 146(3):359–388

Freire FG, Davies LC, Vacas AM, Novais JM, Martins-Dias S (2009) Influence of operating conditions on the degradation kinetics of an azo-dye in a vertical flow constructed wetland using a simple mechanistic model. Ecol Eng 35(10):1379–1386

Fu Y, Viraraghavan T (2001) Fungal decolorization of dye wastewaters: a review. Bioresource Technol 79(3):251–262

Fürtig K, Pavelic D, Brunold C, Brändle R (1999) Copper- and iron-induced injuries in roots and rhizomes of reed (*Phragmites australis*). Limnologica 29(1):60–63

Gonzalez-Alcaraz MN, Egea C, Jimenez-Carceles FJ, Parraga I, Maria-Cervantes A, Delgado MJ, Alvarez-Rogel J (2012) Storage of

organic carbon, nitrogen and phosphorus in the soil-plant system of *Phragmites australis* stands from a eutrophicated Mediterranean salt marsh. Geoderma 185:61–72

Ha CV, Leyva-González ML, Osakabe Y, Tran UT, Nishuyama R, Watanabe Y, Tanaka M, Seki M, Yamaguchi S, Dong NV, Yamaguchi-Shinozaki K, Shinozaki K, Herrera-Estrella L, Tran LP (2014) Positive regulatory role of strigolactone in plant responses to drought and salt stress. Proc Natl Acad Sci 111(2):851–856

Habig WH, Pabst MJ, Jakoby WB (1974) Glutathione S-transferases. The first enzymatic step in mercapturic acid formation. J Biol Chem 249(22):7130–7139

Havaux M (1998) Carotenoids as membrane stabilizers in chloroplasts. Trends Plant Sci 3(4):147–151

Kalra YP (ed) (1998) Handbook of reference methods for plant analysis. CRC Press, Taylor & Francis Group, Boca Raton

Kaushik P, Malik A (2009) Fungal dye decolourization: recent advances and future potential. Environ Int 35(1):127–141

Khataee AR, Movafeghi A, Torbati S, Lisar SYS, Zarei M (2012) Phytoremediation potential of duckweed (*Lemna minor L.*) in degradation of CI Acid Blue 92: Artificial neural network modeling. Ecotox Environ Safe 80:291–298

Kiba T, Kudo T, Kojima M, Sakakibara H (2011) Hormonal control of nitrogen acquisition: roles of auxin, abscisic acid, and cytokinin. J Exp Bot 62(4):1399–1409

Kim J-S, Yun B-W, Choi JS, Kim T-J, Kwak S-S, Cho K-Y (2004) Death mechanisms caused by carotenoid biosynthesis inhibitors in green and in undeveloped plant tissues. Pestic Biochem Physiol 78(3): 127–139

Kissen R, Winge P, Tran DH, Jørstad TS, Størseth TR, Christensen T, Bones AM (2010) Transcriptional profiling of an Fd-GOGAT1/GLU1 mutant in *Arabidopsis thaliana* reveals a multiple stress response and extensive reprogramming of the transcriptome. BMC Genomics 11:190

Korte F, Kvesitadze G, Ugrekhelidze D, Gordeziani M, Khatisashvili G, Buadze O, Zaalishvili G, Coulston F (2000) Organic toxicants and plants. Ecotox Environ Safe 47(1):1–26

Lichtenthaler HK (1987) Chlorophylls and carotenoids: pigments of photosynthetic biomembranes. Methods Enzymol 148:350–382

Lippert I, Rolletschek H, Kohl J-G (2001) Photosynthetic pigments and efficiencies of two *Phragmites australis* stands in different nitrogen availabilities. Aquat Bot 69(2–4):359–365

Martins Dias S (1998) Tratamento de efluentes em zonas húmidas construídas ou leitos de macrófitas. Bol Biotecnol 60:14–20, http://www.spbt.pt/boletim.aspx

May JM, Mendiratta S, Hill KE, Burk RF (1997) Reduction of dehydroascorbate to ascorbate by the selenoenzyme thioredoxin reductase. J Biol Chem 272(36):22607–22610

Mittler R (2002) Oxidative stress, antioxidants and stress tolerance. Trends Plant Sci 7(9):405–410

Miyake C, Asada K (1996) Inactivation mechanism of ascorbate peroxidase at low concentrations of ascorbate; hydrogen peroxide decomposes compound I of ascorbate peroxidase. Plant Cell Physiol 37(4): 423–430

Mockett RJ, Sohal RS, Orr WC (1999) Overexpression of glutathione reductase extends survival in transgenic *Drosophila melanogaster* under hyperoxia but not normoxia. FASEB J 13(13):1733–1742

Noctor G, Foyer CH (1998) Ascorbate and glutathione: keeping active oxygen under control. Annu Rev Plant Physiol Plant Mol Biol 49: 249–279

Novais J, Martins-Dias S (2003) Constructed wetlands for industrial wastewater treatment contaminated with nitroaromatic organic compounds and nitrate at very high concentrations. 1st International Seminar on The use of Aquatic Macrophytes for Wastewater Treatment in constructed wetlands 277–288

Ogawa K, Hatano-Iwasaki A, Yanagida M, Iwabuchi M (2004) Level of glutathione is regulated by ATP-dependent ligation of glutamate and cysteine through photosynthesis in *Arabidopsis thaliana*: mechanism of strong interaction of light intensity with flowering. Plant Cell Physiol 45(1):1–8

Patil RT, Speaker TJ (2000) Water-based microsphere delivery system for proteins. J Pharm Sci 89(1):9–15

Pearce CI, Lloyd JR, Guthrie JT (2003) The removal of colour from textile wastewater using whole bacterial cells: a review. Dyes Pigm 58(3):179–196

Potters G, De Gara L, Asard H, Horemans N (2002) Ascorbate and glutathione: guardians of the cell cycle, partners in crime? Plant Physiol Biochem 40(6–8):537–548

Pradhan A, Sahu SK, Dash AK (2013) Changes in pigment content (chlorophyll and carotenoid), enzyme activities (catalase and peroxidase), biomas and yield of rice plant (*Oriza sativa L*) following irrigation of rice mill wastewater under pot culture conditions. Int J Sci Eng Res 4(6):2706–2718

Quan LJ, Zhang B, Shi WW, Li HY (2008) Hydrogen peroxide in plants: a versatile molecule of the reactive oxygen species network. J Integr Plant Biol 50(1):2–18

Rad AM, Ghourchian H, Moosavi-Movahedi AA, Hong J, Nazari K (2007) Spectrophotometric assay for horseradish peroxidase activity based on pyrocatechol-aniline coupling hydrogen donor. Anal Biochem 362(1):38–43

Rizhsky L, Hallak-Herr E, Van Breusegem F, Rachmilevitch S, Barr JE, Rodermel S, Inzé D, Mittler R (2002) Double antisense plants lacking ascorbate peroxidase and catalase are less sensitive to oxidative stress than single antisense plants lacking ascorbate peroxidase or catalase. Plant J 32(3):329–342

Rochaix JD (2011) Regulation of photosynthetic electron transport. Biochim Biophys Acta 1807(8):878–886

Saratale RG, Saratale GD, Chang JS, Govindwar SP (2011) Bacterial decolorization and degradation of azo dyes: a review. J Taiwan Inst Chem Eng 42(1):138–157

Scandalios JG, Guan L, Polidoros AN (1997) Catalases in plants: gene structure, properties, regulation, and expression. Oxidative stress and the molecular biology of antioxidant defenses. Liboratory Press, Cold Spring Harbor

Schröder P, Scheer CE, Diekmann F, Stampfl A (2007) How plants cope with foreign compounds—translocation of xenobiotic glutathione conjugates in roots of barley (*Hordeum vulgare*). Environ Sci Pollut R 14(2):114–122

Schwitzguébel JP, Page V, Martins-Dias S, Davies LC, Vasilyeva G, Strijakova E (2011) Using plants to remove foreign compounds from contaminated water and soil in organic xenobiotics and plants: from mode of action to ecophysiology. Springer Science Business Media B.V, Dordrecht

Shaffiqu TS, Roy JJ, Nair RA, Abraham TE (2002) Degradation of textile dyes mediated by plant peroxidases. Appl Biochem Biotechnol 102: 315–326

Solís M, Solís A, Pérez HI, Manjarrez N, Flores M (2012) Microbial decolouration of azo dyes: a review. Process Biochem 47(12):1723–1748

van der Zee FP, Villaverde S (2005) Combined anaerobic–aerobic treatment of azo dyes—A short review of bioreactor studies. Water Res 39(8):1425–1440

Velikova V, Loreto F (2005) On the relationship between isoprene emission and thermotolerance in *Phragmites australis* leaves exposed to high temperatures and during the recovery from a heat stress. Plant Cell Environ 28(3):318–327

Velikova V, Pinelli P, Loreto F (2005) Consequences of inhibition of isoprene synthesis in *Phragmites australis* leaves exposed to elevated temperatures. Agric Ecosyst Environ 106(2–3): 209–217

Vishnevetsky M, Ovadis M, Vainstein A (1999) Carotenoid sequestration in plants: the role of carotenoid-associated proteins. Trends Plant Sci 4(6):232–235

Xu J, Zhang J, Xie H, Li C, Bao N, Zhang C, Shi Q (2010) Physiological responses of *Phragmites australis* to wastewater with different chemical oxygen demands. Ecol Eng 36(10):1341–1347

Yoo SD, Greer DH, Laing WA, McManus MT (2003) Changes in photosynthetic efficiency and carotenoid composition in leaves of white clover at different developmental stages. Plant Physiol Biochem 41(10):887–893

Zang J, Kirkham MB (1996) Enzymatic responses of the ascorbate-glutathione cycle to drought in sorghum and sunflower plants. Plant Sci 113:139–147

Zemlin R, Kühl H, Kohl J-G (2000) Effects of seasonal temperature on shoot growth dynamics and shoot morphology of common reed (*Phragmites australis*). Wetl Ecol Manag 8(6):447–457